

Deep learning-based species-area models reveal multi-scale patterns of species richness and turnover

Victor Boussange^{1,*}, Philipp Brun¹, Johanna T. Malle^{1,2}, Gabriele Midolo³, Jeanne Portier⁴,
Théophile Sanchez^{5,6}, Niklaus E. Zimmermann¹, Irena Axmanová⁷, Helge Bruelheide^{8,9}, Milan
Chytrý⁷, Stephan Kambach⁸, Zdeňka Lososová⁷, Martin Večeřa⁷, Idoia Biurrun¹⁰, Klaus T. Ecker¹¹,
Jonathan Lenoir¹², Jens-Christian Svenning¹³, Dirk Nikolaus Karger¹

¹ Dynamic Macroecology, Land Change Science, Swiss Federal Research Institute WSL, CH-8903 Birmensdorf, Switzerland

² Department of Evolutionary Biology and Environmental Studies, University of Zurich, Zurich, Switzerland

³ Department of Spatial Sciences, Faculty of Environmental Sciences, Czech University of Life Sciences Prague, Praha - Suchdol, Czech Republic

⁴ Resource Analysis, Forest Resources and Management, Swiss Federal Research Institute WSL, CH-8903 Birmensdorf, Switzerland

⁵ Ecosystems and Landscape Evolution, Department of Environmental Systems Science, ETH Zürich, Zürich, Switzerland

⁶ Ecosystems and Landscape Evolution, Land Change Science, Swiss Federal Research Institute WSL, CH-8903 Birmensdorf, Switzerland

⁷ Department of Botany and Zoology, Faculty of Science, Masaryk University, Brno, Czech Republic

⁸ Institute of Biology, Geobotany and Botanical Garden, Martin Luther University Halle-Wittenberg, Halle (Saale), Germany

⁹ German Centre for Integrative Biodiversity Research (iDiv) Halle-Jena-Leipzig, Leipzig, Germany

¹⁰ Department of Plant Biology and Ecology, Faculty of Science and Technology, University of the Basque Country UPV/EHU, Bilbao, Spain

¹¹ Ecosystem Dynamics, Biodiversity and Conservation Biology, Swiss Federal Research Institute WSL, CH-8903 Birmensdorf, Switzerland

¹² UMR CNRS 7058 'Ecologie et Dynamique des Systèmes Anthropisés' (EDYSAN), Université de Picardie Jules Verne, F-80037 Amiens, France

¹³ Center for Ecological Dynamics in a Novel Biosphere (ECONOVO), Aarhus University, DK-8000 Aarhus C, Denmark

* Corresponding author, email: vic.boussange@gmail.com

July 10, 2025

Abstract

The number of species within ecosystems is influenced not only by their intrinsic characteristics but also by the spatial scale considered. As the sampled area expands, species richness increases, a phenomenon described by the species-area relationship (SAR). The accumulation dynamics of the SAR results from a complex interplay of biotic and abiotic processes operating at various spatial scales. However, the challenge of collecting exhaustive biodiversity records across spatial scales has hindered a comprehensive understanding of these dynamics. Here, we develop a deep learning approach that leverages sampling theory and small-scale ecological surveys to spatially resolve the scale-dependency of species richness. We demonstrate its performance by predicting the species richness of vascular plant communities across Europe, and evaluate the predictions against an independent dataset of plant community inventories. Our model improves species richness estimates by 32% and delivers spatially explicit patterns of species richness and turnover for sampling areas ranging from square meters to hundreds of square kilometers. Explainable AI techniques further disentangle how drivers of species richness operate across spatial scales. The ability of our model to represent the multi-scale nature of biodiversity is essential to deliver robust biodiversity assessments and forecasts under global change.

Contents

| | | |
|-----------|--|-----------|
| 1 | Introduction | 2 |
| 2 | Results | 3 |
| 2.1 | Model performance | 3 |
| 2.2 | Contribution of area and environment across spatial scales | 5 |
| 2.3 | Scale-specific patterns of plant species richness and turnover in Europe | 6 |
| 3 | Discussion | 9 |
| 4 | Conclusion | 10 |
| 5 | Methods | 10 |
| 5.1 | Problem statement | 10 |
| 5.2 | Deep SAR model | 11 |
| 5.3 | Data | 12 |
| 6 | Data availability | 12 |
| 7 | Code availability | 12 |
| 8 | Author contributions | 12 |
| 9 | Acknowledgements | 13 |
| S1 | Supplementary materials | 19 |
| S2 | Supplementary figures | 19 |

1 Introduction

Biodiversity is experiencing unprecedented changes due to global change stressors (IPBES, 2019), with impacts that critically vary across spatial scales (Smart et al., 2006). Agriculture, for example, can increase local diversity through biotic homogenization, but causes biodiversity loss at regional scales by degrading natural habitats (Fahrig, 1997; Maxwell et al., 2016; Simkin et al., 2022; Keil et al., 2015). Similarly, climate change drives divergent richness patterns across spatial scales by altering species distributions and community assembly processes (IPBES, 2019). Assessing how diversity responds to global change across spatial scales is therefore crucial for evaluating the state and trends of biodiversity (Powers and Jetz, 2019; Newbold, 2018; He and Hubbell, 2011). Yet, scaling up small-scale effects from local to regional levels poses a major challenge, resulting in a critical knowledge gap (IPBES et al., 2018).

The species-area relationship (SAR) is a key concept to comprehend biodiversity patterns across spatial scales. Here, we use the term "spatial scale" broadly to designate the sampling area, study extent, spatial resolution, or spatial grain, *sensu* O'Neill (1986). Traditionally expressed as a power law, $S = cA^z$ (Arrhenius, 1921), the SAR describes how species richness S increases with sampling area A . The parameter c represents the species richness observed within a unit area, commonly referred to as α -diversity. z determines the slope of the SAR on a log-log scale (i.e., the derivative of $\log S$ w.r.t $\log A$), with higher z values indicating a faster accumulation of species with area. z is often associated with the concept of β -diversity, or species turnover (see Matthews et al. (2021a); Halley et al. (2013); Whittaker and Fernández-Palacios (2007); Triantis et al. (2012), although these terms have alternative definitions (Tuomisto, 2010)). The SAR permits therefore to scale-up local α -diversity to estimate regional species richness, also known as γ -diversity. By allowing the prediction of biotic diversity across full range of ecologically relevant spatial scales, the SAR is instrumental for a comprehensive estimation of species richness.

While the power-law SAR model is a convenient formulation, it relies on the strong assumption of a linear relationship between area and species richness on a log-log scale, which may be considered only valid for a limited range of scenarios

and spatial scales (Dengler, 2009; Guilhaumon et al., 2008). In reality, the accumulation of species richness changes in a non-linear fashion as different environmental drivers and ecological barriers are encountered at increasingly larger spatial extents (Conor and McCoy (2013); Borda-de-Água et al. (2012)). As a consequence, the SAR is also location-specific, and depends on biotic and abiotic factors within the area considered (Betts et al. (2014); Matthews et al. (2016); He and Legendre (2002)). Drivers, such as climate, topography, soil conditions, and habitat type shape the spatial distribution of species, affecting the rate at which they accumulate (He and Legendre, 2002; He and Hubbell, 2011; Weigelt and Kreft, 2013; Matthews et al., 2021b; Borda-de-Água et al., 2012; Ulrich et al., 2022; Drakare et al., 2006). Importantly, the effect of these drivers is also scale dependent (Willis and Whittaker, 2002; Turner and Tjørve, 2005; Wiens, 1989).

A number of studies have characterized the effect of environmental drivers on the SAR (Turner and Tjørve, 2005). One branch of research has relied on species inventories from islands or political units to investigate these effects. For instance, Triantis et al. (2003); Kallimanis et al. (2008) showed that incorporating habitat heterogeneity into SAR models better captures spatial variations in species richness, while Kalmar and Currie (2007) extended a power law SAR model by incorporating climate-species interactions to predict global bird species richness. However, the coarse spatial scales of these units limits the characterization of subtle differences in SAR arising at finer spatial grains. Another line of research has focused on developing methods to estimate the SAR from small-scale ecological surveys, some of which are reviewed in (Kunin et al., 2018). These methods are based on sampling theory, which, through explicit or implicit assumptions about the species density distribution, predicts the expected species richness given a certain sampling effort (Elena Schmitz and Rahmann, 2025). Notably, Portier et al. (2022) used small-scale plots that were incrementally aggregated within political units to build country-specific rarefaction curves, predicting expected observed species richness for a given sampling effort. These curves were fitted with a simple statistical model parameterized by environmental features to produce standardized tree-species richness assessments. With a sufficiently expressive statistical model, we could generalize this method to enable the prediction of location and area-specific rarefaction curves. Extrapolating these rarefaction curves to infinite sampling effort could enable the prediction of spatially explicit variations in species richness across spatial scales (Chao et al., 2014; SoberónM. and LlorenteB, 1993; Gotelli and Colwell, 2001).

Here, we present a deep learning approach that leverages small-scale ecological surveys and sampling theory to predict spatially explicit SARs. Specifically, we train a deep neural network to predict the rarefaction curve expected within a spatial unit based on its area and environmental characteristics (see Fig. 1 for an illustration). The neural network parametrizes an asymptotic statistical model that predicts expected species richness for a given sampling effort. By extrapolating this statistical model to its asymptote, we can estimate total species richness within the spatial unit under consideration. We formally justify this approach using sampling theory in Methods. Since our model predicts total species richness within spatial units of arbitrary area, we refer to it as a deep SAR model. We train our deep SAR model using 400k vegetation plots from the European Vegetation Archive, comprising 9,480 distinct species (EVA, Chytrý et al. (2016)), to predict vascular plant species richness across Europe. We evaluate the model’s extrapolation performance using an independent dataset of regional plant inventories from the GIFT database (Weigelt et al., 2020). For environmental features, we calculate the mean and standard deviation of seven bioclimatic variables within each spatial unit, characterizing both mean environmental conditions and environmental heterogeneity. We consider three model variants trained with area only, environmental features only, or both, to systematically evaluate their contributions to predicting species richness. We benchmark our deep SAR model against a traditional non-parametric species richness estimator, and employ Shapley value analysis to disentangle how environmental drivers influence species richness across spatial scales. Finally, we demonstrate the model’s capacity to generate spatially explicit maps of plant species richness and turnover across Europe at multiple spatial scales, revealing the multi-scale aspect of biodiversity patterns that traditional approaches cannot capture.

2 Results

2.1 Model performance

The deep SAR model demonstrated superior performance in interpolating across location and area-specific species rarefaction curves when utilizing environmental features (Fig. 2a). To evaluate the models’ performance, we used held-out vegetation plots (see Biodiversity data for details on the training and test datasets), assessing their capacity to predict species rarefaction curves for low to moderate sampling effort. We trained the deep SAR using three sets of features: area

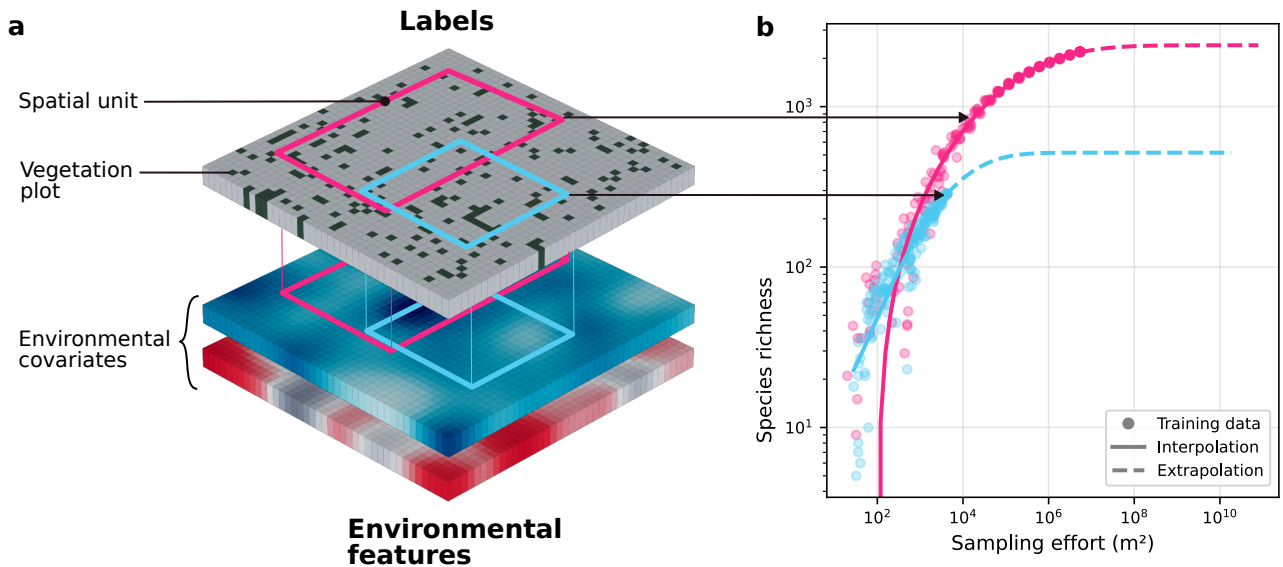


Figure 1: **Deep learning approach for predicting location and area-specific rarefaction curves from small-scale ecological surveys.** (a) Data preparation and feature extraction. The top layer shows the location of ecological surveys, which are randomly pooled within spatial units of varying sizes and locations (blue and red boxes) to construct location and area-specific rarefaction curves. The bottom layers show environmental covariates, which we use to derive features characterising the spatial units. (b) Location and area-specific species rarefaction estimation. For each spatial unit, subsampled species counts (scatter points) are fitted with an asymptotic statistical model, which we extrapolate to estimate the total expected species richness under infinite sampling effort. We justify this approach with sampling theory (see Methods for details). A deep neural network learns to predict the parameters of this asymptotic statistical model based on the spatial unit environmental features, enabling the estimation of the rarefaction curve for any location and spatial extent, and the prediction of species richness over increasing area. In practice, we only generate one subsampled species count per spatial unit, but many more spatial units, to span large extents efficiently.

only, environmental features only, and both area and environmental features. Following Kunin et al. (2018), we employed the root mean squared error (RMSE) to evaluate model performance, measured across five independent training runs. Providing the deep SAR model with statistics on environmental features reduced the RMSE on the EVA test dataset by 43% compared to using area only. The performance of the model informed with both area and environmental features was not significantly improved compared to the model trained with environmental features only. This can be attributed to the high correlation between the standard deviations of environmental features and the spatial unit area (see correlation matrix in Fig. S7). The best models showed a median relative bias of -19% in predicting the species rarefaction curves on the EVA-based test dataset (Fig. 2b), indicating a moderate tendency to overpredict species richness. This bias was more pronounced for low values of species richness and decreased as species richness increased.

The model trained with both area and environmental features together demonstrated the best performance in extrapolating to predict total species richness. Total species richness was obtained by extrapolating the predicted rarefaction curve towards its asymptote, assuming infinite sampling effort. We matched these predictions against species richness derived from species inventories obtained from the GIFT database. Overall, the best extrapolating model was the one leveraging both area and environmental features. The RMSE of this model was 23% lower than that of the model trained with area only. Contrary to its interpolation performance, we found a significant advantage in using area together with environmental features over environmental features only (performance gain of 12%, p -value < 0.001 under t-test). The

improved performance provided by the sampling unit area can be interpreted as an effect of "area *per se*" (Connor and McCoy, 1979). Along this mechanism, larger areas promote higher species richness, even when discounting for increased diversity in environmental niches, as they increase the population size, allowing more individuals to be sampled, and as they bridge barriers to dispersal (Drakare et al., 2006). We note that the distribution of data points in the GIFT dataset is biased towards larger areas (in the order of magnitude of a country's area, see Fig. S6). At this scale, the summary statistics of environmental features used to inform the model are less informative than for smaller areas (see Contribution of area and environment across spatial scales and Fig. 3) and where species richness shows less variation. We expect that more fine-grained data points or the use of higher-order summary statistics for the environmental features would give a larger advantage to the deep SAR model trained with environmental features.

Last but not least, the deep SAR model significantly outperformed the Chao2 estimator on extrapolation performance (gain of 32%, p -value < 0.001 under t-test) and provided comparably less biased estimates of species richness (median relative bias of 22% compared to 52% for the Chao2 estimator).

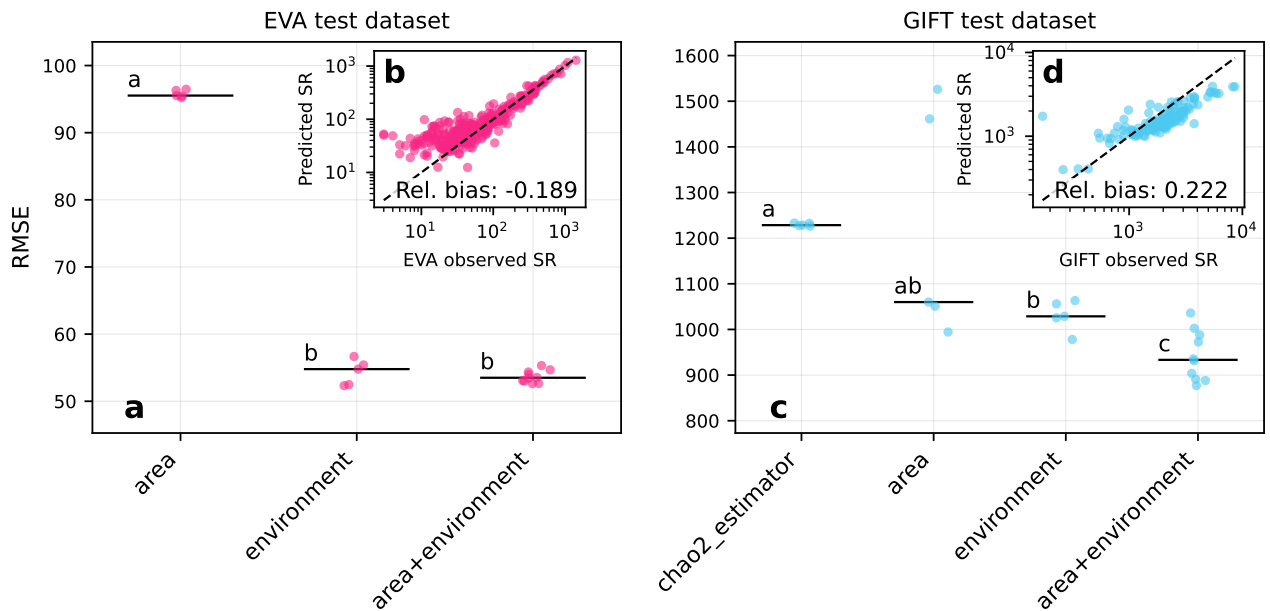


Figure 2: **Ablation study and performance evaluation of the deep SAR model.** (a) Interpolation performance of the deep SAR model for low to moderate sampling effort, as measured by the root mean squared error (RMSE), trained with each set of features, on the held-out plot vegetation test dataset. Different lower letters above the boxplots indicate that performance are significantly different from each other (Posthoc Tukey HSD test). (b) Observed species richness against values predicted by the best model (area + environment). (c) Extrapolation performance of the deep SAR model, trained with each set of features, and compared against the non-parametric Chao2 estimator, on the GIFT-based test dataset. (d) Observed species richness against values predicted by the best model (area + environment).

In summary, these results suggest that (i) our model effectively predicts the rarefaction curves associated with spatial units of arbitrary location and extent, providing the expected species richness given a certain sampling effort, and (ii) reliably extrapolates to predict total species richness. Hence, the proposed approach successfully accounts for variations in SAR due to environmental drivers, capturing species richness patterns across scales.

2.2 Contribution of area and environment across spatial scales

Disentangling the effect of spatial unit area on species richness from environmentally-related confounding factors has been a challenging task in macroecology, as these factors act differently depending on spatial scale. To quantify the relative contributions of environmental features versus area, we calculated the relative Shapley values (Lundberg and Lee,

2017) for each predictor class (area of the spatial unit considered, mean and heterogeneity of environmental conditions), stratified by sampling area. Specifically, we calculated absolute Shapley values for each predictor class and normalized them so that the sum of Shapley values for all features equals one for each prediction of species richness. This approach allows us to characterize the relative importance of each predictor class across varying sampling areas, as shown in Fig. 3.

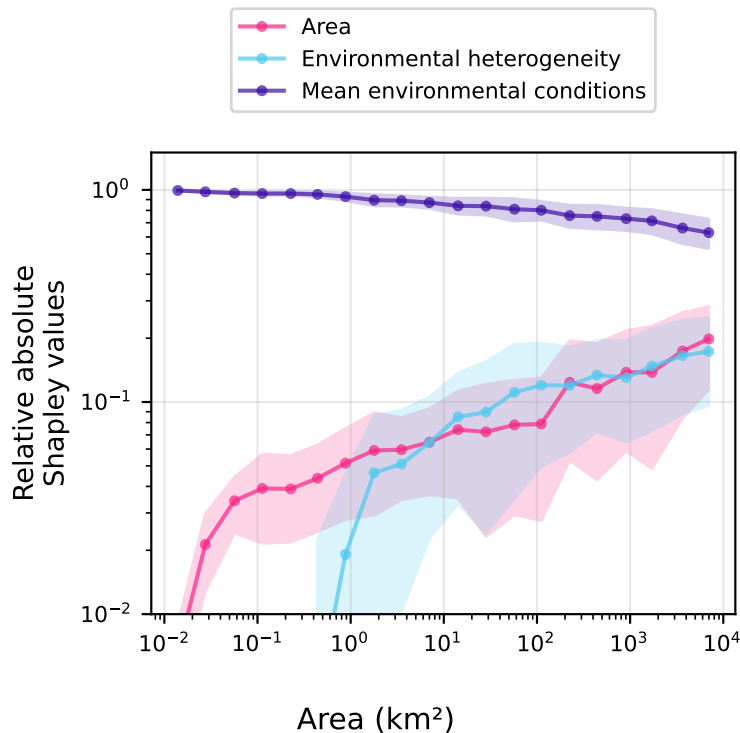


Figure 3: **Relative importance of area and environmental conditions in predicting species richness.** This plot shows the relative importance as indicated by Shapley values for the spatial unit area and environmental features, grouped into two classes: mean environmental conditions and environmental heterogeneity. Higher values indicate a greater contribution of the respective predictor group to predicting species richness at any given spatial grain. Plain lines indicate the mean relative absolute Shapley values across all predictions, while shaded areas represent the standard deviation.

Mean environmental conditions were the dominant drivers of species richness across all spatial scales investigated. This finding supports the environmental filtering hypothesis, wherein mean environmental conditions constrain species richness by limiting species establishment based on physiological tolerances (Whittaker, 1972; Rahbek, 2005). As the spatial unit area increases, the relative contributions of both area and environmental heterogeneity increased, while the influence of mean environmental conditions decreased. Environmental heterogeneity promotes higher species richness by increasing niche diversity, which supports greater species turnover (Stein et al., 2014; Qian and Ricklefs, 2012; Turner and Tjørve, 2005). Meanwhile, larger sampling areas can enhance species richness by allowing more individuals to be sampled ("area *per se*" effect, see previous section). We note that habitat area is strongly correlated with the standard deviation of bioclimate variables in our dataset (see Fig. S7), which may confound the interpretation of area effects versus environmental heterogeneity. These findings quantify the scale-dependent nature of biodiversity drivers (Rahbek, 2005) and provide quantitative evidence for the mechanisms underlying species richness patterns across spatial scales (Field et al., 2009).

2.3 Scale-specific patterns of plant species richness and turnover in Europe

Projections of species richness and turnover across spatial scales are essential for comparing biodiversity trends from local to regional levels. Given the superior performance of the deep SAR model informed with location and area-specific environmental features, we used it to map species richness and turnover across Europe at multiple spatial scales. We defined turnover as the slope of the SAR predicted at each location ($\frac{dS}{dA}$). Using a moving window approach with different spatial grains, we derived environmental features that served as predictors to estimate species richness at the centroid of each window. We also estimated location-specific SARs for three environmentally distinct locations by incrementally increasing the area of spatial units centered at each location of interest.

The model revealed markedly different patterns of species richness across spatial scales. At fine spatial scales (1 km), mountainous areas exhibited relatively lower species richness compared to lowland regions (Fig. 4b), contrary to established biogeographical knowledge of European vascular plant diversity (Cai et al., 2023). However, predictions at coarser spatial scales (50 km) revealed the expected highest species richness along the Mediterranean coastline and in mountainous regions including the Alps, Carpathians, and Dinarides (Fig. 4c). This scale-dependent variation underscores the critical importance of considering spatial grain in macroecological analyses (Wiens, 1989; Portier et al., 2022).

The predicted location-specific SARs explicitly encapsulated these scale-dependent dynamics (Fig. 4a). The South-western Alps (blue curve) exhibited lower local species richness at fine spatial scales compared to the Northern Iberian Peninsula (purple curve) and Northern Germany (red curve). However, as spatial scale increases, species richness in the Alps surpasses both other locations due to higher species turnover. This pattern reflects the characteristic biodiversity structure of mountain environments, where lower local carrying capacity is offset by higher niche diversity driven by environmental heterogeneity, resulting in low local richness but high species turnover and regional richness (Antonelli et al., 2018). The geographic variations in species turnover reflected these patterns (Fig. 4d-e). Notably, turnover patterns differed substantially from species richness patterns at fine scales. Mountain environments showed moderate species richness but high turnover, which effectively translated into higher species richness at coarser scales.

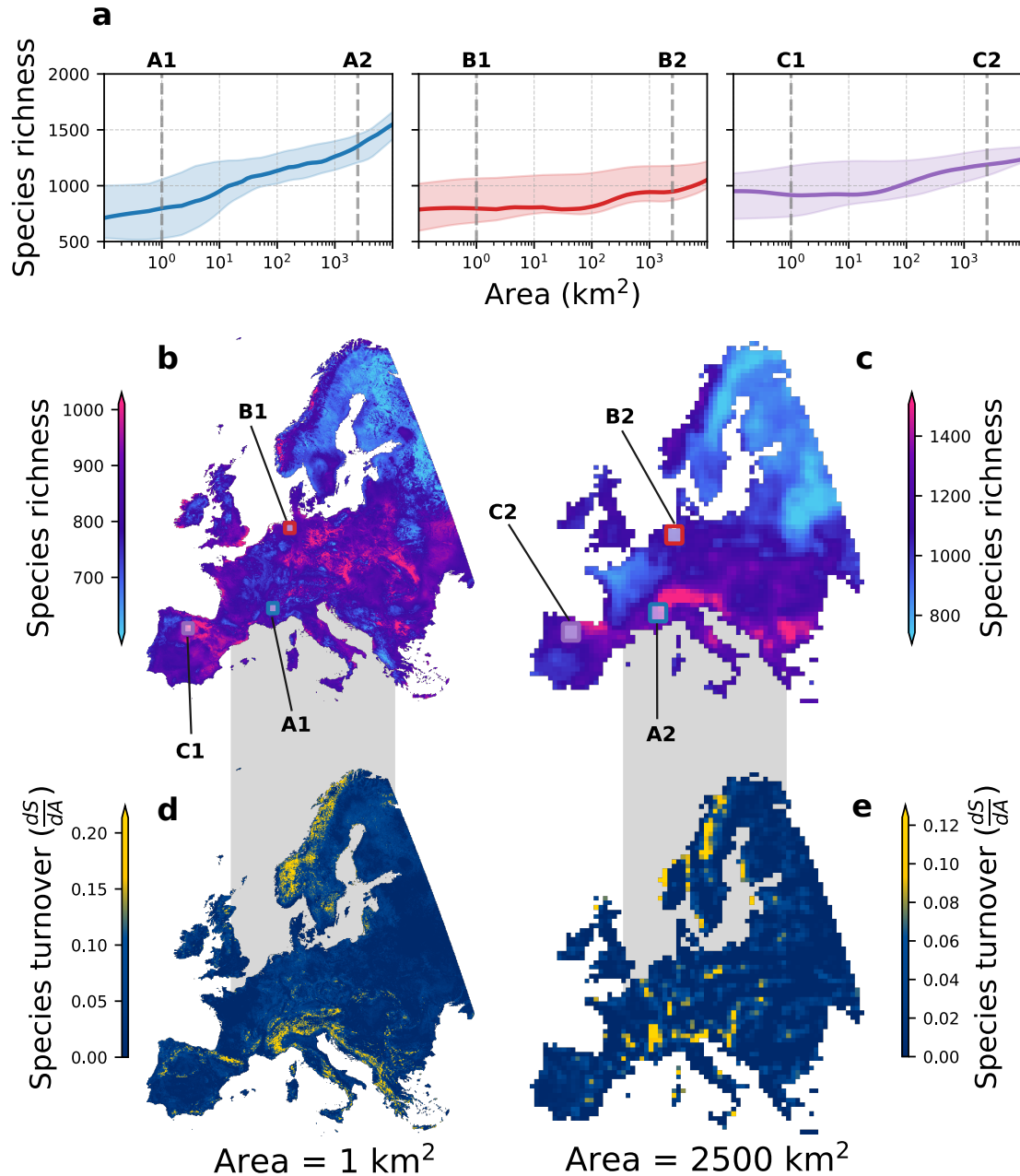


Figure 4: **Species richness and turnover across Europe, predicted at multiple spatial scales.** (a) Predicted SARs for three distinct locations, as indicated in panels (b) and (c). Plain lines represent the mean while shaded areas indicate the standard deviation of the predictions derived from the ensemble model. (b-c) Maps of species richness obtained for square spatial units with edge lengths of 1 km and 50 km, respectively. (d-e) Associated maps of species turnover. Species turnover is defined as the slope of the SAR predicted at each location.

3 Discussion

Our deep SAR model successfully predicted species rarefaction curves across spatial units of varying locations and areas by leveraging environmental features, allowing to predict location-specific species area relationships under asymptotic sampling effort. By predicting species rarefaction curves in environmental space, our approach leverages well-sampled regions to make predictions in environmentally similar but less-surveyed areas. This represents a significant advantage over conventional non-parametric estimators that rely solely on local incidence data without incorporating environmental context. Consequently, our model achieved a 32% improvement over the Chao2 estimator when predicting total species richness. Environmental features proved critical for model performance, reducing prediction error by 43% compared to area-only models. Shapley value analysis revealed that environmental conditions are the primary drivers of species richness across all spatial scales, while highlighting the increasing relative importance of area effects and environmental heterogeneity at larger spatial grains. Spatially explicit predictions of species richness and turnover uncovered scale-dependent biodiversity patterns, with Mediterranean coastlines and mountainous regions exhibiting highest species richness at coarse scales, despite mountainous areas showing relatively lower local richness at fine scales. These results collectively demonstrate that our approach can effectively capture the multi-scale relationships between environmental drivers and species richness patterns.

The application of machine learning in quantitative ecology has predominantly focused on predicting species distributions (Brun et al., 2024). However, many ecological and conservation questions require understanding macroecological properties at the community or ecosystem level. Our deep SAR model adopts a fundamentally different approach by directly modeling community-level biodiversity patterns rather than individual species distributions. By capturing how environmental conditions influence species richness accumulation across spatial scales without explicitly modeling individual species' ranges, our approach offers several advantages. First, it is more data-efficient as it leverages the aggregated signal from multiple species rather than requiring sufficient data for each species individually. Second, it can exploit general relationships between environmental heterogeneity and species richness that remain consistent across biogeographic regions (Leroux et al., 2017; Dubuis et al., 2011). This enhances model transferability and generalization compared to species distribution models, which often suffer from limited occurrence data, particularly for rare species, and may not capture emergent community-level properties that arise from species interactions and assembly processes.

The theoretical functional form of the SAR has long been debated in ecology, with no consensus on the most appropriate model (Dengler, 2009). While the search for appropriate functional forms is crucial in low-data regimes where strong inductive bias is required, theoretical forms are simplifications that cannot accommodate the complexity of realistic landscapes. Within local species communities, species richness is expected to increase smoothly as sampling area grows, reflecting saturation of local species pools (Connor and McCoy, 1979; Hubbell, 2001). However, as sampling area expands to include neighboring distinct communities, species numbers may rise sharply due to incorporation of novel species assemblages (Whittaker, 1972; Gering et al., 2003). By leveraging abundant small-scale ecological survey data, we can employ more flexible deep neural networks to capture these complex dynamics without imposing strong assumptions about functional form. These models have the capacity to express nonlinear dynamics occurring across dispersal barriers and in response to complex natural or anthropogenic drivers across the full range of ecologically relevant scales.

Our deep SAR model provides a comprehensive framework for biodiversity assessment and conservation planning by quantitatively evaluating environmental driver effects on species richness across spatial scales. For instance, our deep SAR model could enable habitat loss impact assessment by comparing predicted species richness between intact and degraded areas (Gotelli and Colwell, 2001; Matthews et al., 2021a; Thomas et al., 2004; Brooks et al., 2002), while capturing scale-dependent effects often overlooked in traditional assessments. Species turnover maps offer particularly valuable conservation insights. High-turnover regions indicate rapid species richness increase with area, suggesting that habitat loss may disproportionately impact regional biodiversity by eliminating unique assemblages (Socolar et al., 2016). Conversely, areas with high local richness but low turnover may exhibit greater resilience to localized habitat loss, harboring species pools less dependent on large-scale environmental gradients. Explainable AI methods, such as Shapley values, quantify how environmental stressor effects on species richness vary across spatial scales, therefore allowing to enhance our understanding of biodiversity responses. The multi-scale capability of our model delivers critical information that can match the spatial scale of conservation objectives (Kunin et al., 2018).

From a machine learning perspective, predicting species richness from pools of ecological surveys represents a multiple instance learning (MIL) problem (Carbonneau et al., 2018). Ecological surveys correspond to instances, their aggregation generates training samples (bags), and predicting species richness involves predicting bag-level labels from

instance-specific (sampling effort) and bag-specific (environmental covariates) features. With this perspective, modern MIL architectures using attention mechanisms could potentially improve species richness estimates (Ilse et al., 2018). While we manually engineered environmental features by calculating means and standard deviations, convolutional neural networks or vision transformers could automatically extract higher-order statistics and leverage satellite imagery to characterize habitat fragmentation effects (Hanski et al., 2013; Rybicki and Hanski, 2013). Future improvements could leverage higher-resolution climate data to capture microenvironmental factors shaping local species assemblages (Dem-bicz et al., 2021), incorporate alternative biodiversity data sources such as citizen science species occurrence data (GBIF: The Global Biodiversity Information Facility, 2022), and extend predictions to other biodiversity metrics including Hill numbers that generalize species richness (Chao et al., 2014) or genetic diversity (De Kort et al., 2021). Enhanced uncertainty characterization beyond model ensembling represents another important direction for transparent biodiversity reporting.

4 Conclusion

Our study demonstrates how deep learning can effectively predict macroecological properties by leveraging abundant small-scale ecological survey data and sampling theory. The deep SAR model provides a data-efficient approach that delivers unprecedented insights into biodiversity patterns across spatial scales, revealing how environmental drivers operate differently at local versus regional scales. The model’s capacity to capture multi-scale biodiversity dynamics is essential for attributing biodiversity changes to global change drivers and designing comprehensive conservation strategies that account for the spatial scale-dependency of ecological processes.

5 Methods

5.1 Problem statement

Estimating total species richness from small-scale ecological surveys. We aim to predict the total species richness S_{tot} within a spatial unit of arbitrary location and area. Let $\lambda_j > 0$ denote the density (individuals per unit area) of species $j \in \{1, \dots, S_{\text{tot}}\}$. The probability of observing x_j individuals of species j in an ecological survey of area a follows a Poisson distribution, $P(N_j = x_j | a) = \frac{(\lambda_j a)^{x_j} e^{-\lambda_j a}}{x_j!}$. For M randomly distributed ecological surveys with areas $\{a_i\}_{i=1}^M$, the probability of not detecting species j in survey i is $P(N_j = 0 | a_i) = e^{-\lambda_j a_i}$. Assuming independence across surveys, the probability of detecting species j in at least one of $m \leq M$ randomly selected surveys is

$$1 - \prod_{i=1}^m e^{-\lambda_j a_i} = 1 - e^{-\lambda_j \sum_{i=1}^m a_i}, \quad (1)$$

where $\sum_{i=1}^m a_i$ is the cumulative area of a specific realization of m surveys. Considering the expected cumulative area when sampling m surveys uniformly at random, denoted by $A(m) = \mathbb{E}[\sum_{i=1}^m a_i]$, the expected observed species richness $\mathbb{E}[S_{\text{obs}}(m)]$ in m randomly selected surveys is:

$$\mathbb{E}[S_{\text{obs}}(m)] = \sum_{j=1}^{S_{\text{tot}}} \left[1 - e^{-\lambda_j A(m)} \right]. \quad (2)$$

Assuming species densities $\{\lambda_j\}_{j=1}^{S_{\text{tot}}}$ follow a distribution $f(\lambda)$, where $\int_0^\infty f(\lambda) d\lambda = 1$, we can rewrite Eq. (2) as an expectation over $f(\lambda)$:

$$\mathbb{E}[S_{\text{obs}}(m)] = S_{\text{tot}} \int_0^\infty \left[1 - e^{-\lambda A(m)} \right] f(\lambda) d\lambda = S_{\text{tot}} (1 - \mathcal{L}\{f\}(A(m))), \quad (3)$$

where $\mathcal{L}\{f\}(s) = \int_0^\infty e^{-s\lambda} f(\lambda) d\lambda$ is the Laplace transform of $f(\lambda)$. Equation (3) provides a generic formula describing the rarefaction curve underlying a species assemblage associated with a spatial unit, based on the species density distribution f .

Maximum likelihood estimation of the rarefaction curve. In practice, we do not know the distribution f nor the total species richness S_{tot} . Instead, parametric approaches assume the existence of a functional form $g_{\Theta}(m)$ that is monotonically increasing and exhibits asymptotic behavior, approximating the expected species richness $\mathbb{E}[S_{\text{obs}}(m)]$ for a given number m of randomly selected surveys (SoberónM. and LlorenteB, 1993; Gotelli and Colwell, 2001; Colwell et al., 1997), where Θ represents the model parameters. Estimating the asymptote reduces to finding Θ such that $g_{\Theta}(m)$ accurately reproduces the observed species richness $S_{\text{obs}}(m)$ across various values of m . Given observed species counts $\{S_{\text{obs}}^{(k)}(m_k)\}_{k=1}^K$ from K random subsets of surveys with sizes m_1, \dots, m_K , we can estimate Θ through maximum likelihood estimation. Notably, the choice of model $g_{\Theta}(m)$ implicitly determines an assumption about the distribution of species densities f . For instance, the commonly used Michaelis-Menten model can be derived from Eq. (3) by assuming that species densities follow an exponential distribution (see Derivation of the Michaelis-Menten model from the exponential distribution).

Four parameter Weibull function. A flexible choice for the functional form g_{Θ} is the four-parameter Weibull function (Zou et al., 2023):

$$g_{\Theta}(m) = c + (S_{\text{tot}} - c) (1 - \exp[-(m/e)^b]) \quad (4)$$

where c corresponds to the lower asymptote as $m \rightarrow 0$ (minimum expected species richness), S_{tot} corresponds to the upper asymptote as $m \rightarrow \infty$ (total species richness), b controls the shape parameter determining the rate of species accumulation, and e is the scale parameter representing the characteristic sampling effort. As visually depicted in Fig. 1b, we found that this function provides a good fit for arbitrary rarefaction curves obtained with our dataset.

5.2 Deep SAR model

Parametrization of rarefaction curves. Rarefaction curves are location and area-specific and depend on the environmental characteristics of the spatial unit considered (Dengler and Oldeland, 2010). To predict the species richness S_{obs} of a spatial unit with arbitrary size and location, we condition g_{Θ} on features X associated with the spatial unit, which include its area and statistics of environmental features within the spatial unit. We use a neural network h_{θ} to learn the mapping from the features X to the parameters Θ of the rarefaction curve model g_{Θ} :

$$\Theta = h_{\theta}(X) \quad (5)$$

The predicted species richness for a given sampling effort m is then

$$\mathbb{E}[S_{\text{obs}}(m | X)] = g_{\Theta}(m, X) = g_{h_{\theta}(X)}(m). \quad (6)$$

The neural network h_{θ} is trained by minimizing the loss function:

$$L(\theta) = \sum_{k=1}^K \left[g_{h_{\theta}(X_k)}(m_k) - S_{\text{obs}}^{(k)}(m_k) \right]^2, \quad (7)$$

where $S_{\text{obs}}^{(k)}(m_k)$ represents the observed species richness from m_k randomly selected surveys within spatial unit k with features X_k .

Training data generation. We generated training samples by randomly placing spatial units containing at least two ecological surveys, with log-transformed areas following a uniform distribution between 10^4 and 10^{11} m². Within each spatial unit k of area A_k , we identified the M_k surveys from the EVA database whose coordinates fell within its bounds. We then selected a random subsample of m_k ecological surveys, where m_k followed a log-uniform discrete distribution $m_k \sim \mathcal{U}_{\log}\{2, 3, \dots, M_k\}$. Based on these selected surveys, we calculated the observed species richness $S_{\text{obs}}^{(k)}$, which corresponded to the number of unique species observed across the selected ecological surveys. We assessed how the number of training samples influences model performance and report the results in Fig. S5. Model performance increased with the number of training samples, and we found that the optimal number is on the order of magnitude of the number of surveys used.

Model architecture and hyperparameters. Our deep SAR models employed fully connected multi-layer perceptrons implemented in PyTorch. The network architecture consisted of 6 fully connected layers with 32, 128, 256, 256, 128, and 32 neurons respectively, using leaky ReLU activation functions. Input features included the spatial unit area and the mean and standard deviation of environmental variables within each spatial unit (detailed in Biodiversity data). For ensemble predictions used in Contribution of area and environment across spatial scales and Scale-specific patterns of plant species richness and turnover in Europe, we trained 5 independent models and aggregated their outputs using arithmetic mean. Standard deviations of ensemble predictions are provided in Fig. S9. We used batch sizes of 1024 samples over 100 epochs for training, which we found sufficient for convergence as shown in Fig. S8. We used the Adam optimizer (Kingma and Ba, 2014) with decoupled weight decay regularization (Loshchilov and Hutter, 2019) and a learning rate scheduler with 20-epoch patience and 0.5 decay factor. Data was split into 90% training and 10% validation subsets for both ablation studies and final ensemble models.

5.3 Data

Biodiversity data. We used a dataset of 502,724 vegetation plots from the European Vegetation Archive (Chytrý et al. (2016); <https://euroveg.org/eva-database/version/2023-02-04>; project 172; data retrieved on 27 February 2023). We selected only plots with available area information and coordinate uncertainty less than 1 km. We additionally discarded plots not located on land within Europe and excluded non-vascular taxa from the dataset. Vegetation plots were analyzed without distinction of habitat types. The data filtering resulted in 488,622 vegetation plots for downstream analyses (see Fig. S10). Additionally, we used the Global Inventory of Floristic Taxonomy (GIFT) database (Weigelt et al., 2020), filtered to select records occurring within continental Europe, resulting in 184 exhaustive species records. We harmonized species names between the EVA and GIFT databases following procedures detailed at <https://github.com/vboussange/DeepSAR>. This resulted in the EVA-based dataset comprising 9,480 distinct species, while the GIFT-based dataset comprised 33,729 distinct species.

Environmental features. We calculated environmental features using seven bioclimatic variables from the CHELSA-BIOCLIM+ dataset (Brun et al., 2022): mean annual air temperature (bio1), temperature seasonality (bio4), annual precipitation (bio12), precipitation seasonality (bio15), near-surface wind speed (sfcWind), potential evapotranspiration (pet), and surface downwelling shortwave radiation (rsds). These variables exhibit low pairwise correlations across the geographical extent (Spearman $\rho < 0.5$). The associated mean climate features also show low correlations (Spearman $\rho < 0.55$), whereas climate heterogeneity features display higher but still moderate correlations (Spearman $\rho < 0.75$; see Fig. S7).

6 Data availability

The preprocessed EVA dataset with anonymized species names and the associated GIFT dataset anonymized with the same procedure are available in our GitHub repository at <https://github.com/vboussange/DeepSAR>. The original EVA dataset has restricted access and is available upon request at <https://euroveg.org/eva-database>. Scripts for downloading and processing the GIFT database are included in our GitHub repository. Upon manuscript acceptance, species richness rasters and trained model weights will be made publicly available.

7 Code availability

The code used to train and evaluate the models and generate all figures is available under our GitHub repository at <https://github.com/vboussange/DeepSAR>.

8 Author contributions

V.B., P.B., J.T.M., G.M., J.P., T.S., N.E.Z., and D.N.K. conceived the study. V.B. developed the methodology, implemented the software, and performed the formal analysis. P.B., J.T.M., G.M., J.P., T.S., and D.N.K. contributed to methodological

development. Data were provided by I.A., H.B., M.C., S.K., Z.L., M.V., I.B., K.T.E., J.L., and J.-C.S. V.B. wrote the original draft. All authors contributed to manuscript review and editing. N.E.Z. and D.N.K. acquired funding. D.N.K. supervised the project. Authors are listed alphabetically in the following order: the core team leading the study (V.B., P.B., J.T.M., G.M., J.P., T.S., N.E.Z.), followed by contributors from the FeedBaCks consortium (I.A., H.B., M.C., S.K., Z.L., M.V.) and EVA data custodians (I.B., K.T.E., J.L., J.-C.S.), also alphabetically within each group, and last the senior author.

9 Acknowledgements

This research was funded through the 2019-2020 BiodivERsA joint call for research proposals, under the BiodivClim ERA-Net COFUND program, and with the funding organisations Swiss National Science Foundation SNF (project: FeedBaCks, 193907), the German Research Foundation (DFG BR 1698/21-1, DFG HI 1538/16-1), and the Technology Agency of the Czech Republic (SS70010002). N.E.Z. considers this work a contribution to the SPEED2ZERO Joint Initiative, which received support from the ETH-Board under the Joint Initiatives scheme. J.C.S. considers this work a contribution to Center for Ecological Dynamics in a Novel Biosphere (ECONOVO), funded by Danish National Research Foundation (grant DNR173).

References

- IPBES. Global assessment report on biodiversity and ecosystem services of the Intergovernmental Science-Policy Platform on Biodiversity and Ecosystem Services. Technical report, Zenodo, May 2019. URL <https://zenodo.org/records/6417333>.
- Simon M Smart, Ken Thompson, Robert H Marrs, Mike G Le Duc, Lindsay C Maskell, and Leslie G Firbank. Biotic homogenization and changes in species diversity across human-modified ecosystems. *Proceedings of the Royal Society B: Biological Sciences*, 273(1601):2659–2665, October 2006. ISSN 0962-8452, 1471-2954. doi: 10.1098/rspb.2006.3630.
- Lenore Fahrig. Relative Effects of Habitat Loss and Fragmentation on Population Extinction. *The Journal of Wildlife Management*, 61(3):603–610, 1997. ISSN 0022-541X. doi: 10.2307/3802168.
- Sean L. Maxwell, Richard A. Fuller, Thomas M. Brooks, and James E. M. Watson. Biodiversity: The ravages of guns, nets and bulldozers. *Nature*, 536(7615):143–145, August 2016. ISSN 1476-4687. doi: 10.1038/536143a.
- Rohan D. Simkin, Karen C. Seto, Robert I. McDonald, and Walter Jetz. Biodiversity impacts and conservation implications of urban land expansion projected to 2050. *Proceedings of the National Academy of Sciences*, 119(12): e2117297119, March 2022. doi: 10.1073/pnas.2117297119.
- Petr Keil, David Storch, and Walter Jetz. On the decline of biodiversity due to area loss. *Nature Communications*, 6(1): 8837, November 2015. ISSN 2041-1723. doi: 10.1038/ncomms9837.
- Ryan P. Powers and Walter Jetz. Global habitat loss and extinction risk of terrestrial vertebrates under future land-use-change scenarios. *Nature Climate Change*, 9(4):323–329, April 2019. ISSN 1758-6798. doi: 10.1038/s41558-019-0406-z.
- Tim Newbold. Future effects of climate and land-use change on terrestrial vertebrate community diversity under different scenarios. *Proceedings of the Royal Society B: Biological Sciences*, 285(1881):20180792, June 2018. ISSN 0962-8452, 1471-2954. doi: 10.1098/rspb.2018.0792.
- Fangliang He and Stephen P. Hubbell. Species–area relationships always overestimate extinction rates from habitat loss. *Nature*, 473(7347):368–371, May 2011. ISSN 1476-4687. doi: 10.1038/nature09985.
- IPBES, M. Rounsevell, M. Fischer, A. T. M. Rando, and A. Mader. The IPBES regional assessment report on biodiversity and ecosystem services for Europe and Central Asia. Technical report, Zenodo, March 2018.

- Robert V O'Neill. *A hierarchical concept of ecosystems*. Number 23. Princeton University Press, 1986.
- Olof Arrhenius. Species and Area. *Journal of Ecology*, 9(1):95–99, 1921. ISSN 0022-0477. doi: 10.2307/2255763.
- Thomas J. Matthews, Kostas A. Triantis, and Robert J. Whittaker, editors. *The Species–Area Relationship: Theory and Application*. Ecology, Biodiversity and Conservation. Cambridge University Press, Cambridge, 2021a. ISBN 978-1-108-47707-9. doi: 10.1017/9781108569422.
- John M. Halley, Vasiliki Sgardeli, and Nikolaos Monokrousos. Species–area relationships and extinction forecasts. *Annals of the New York Academy of Sciences*, 1286(1):50–61, 2013. ISSN 1749-6632. doi: 10.1111/nyas.12073.
- Robert J Whittaker and José María Fernández-Palacios. *Island Biogeography: Ecology, Evolution, and Conservation*. Oxford University Press, 2007.
- Kostas A. Triantis, François Guilhaumon, and Robert J. Whittaker. The island species–area relationship: Biology and statistics. *Journal of Biogeography*, 39(2):215–231, 2012. ISSN 1365-2699. doi: 10.1111/j.1365-2699.2011.02652.x.
- Hanna Tuomisto. A diversity of beta diversities: Straightening up a concept gone awry. Part 1. Defining beta diversity as a function of alpha and gamma diversity. *Ecography*, 33(1):2–22, February 2010. ISSN 09067590. doi: 10.1111/j.1600-0587.2009.05880.x.
- Jürgen Dengler. Which function describes the species-area relationship best? A review and empirical evaluation. *Journal of Biogeography*, 36(4):728–744, April 2009. ISSN 03050270, 13652699. doi: 10.1111/j.1365-2699.2008.02038.x.
- François Guilhaumon, Olivier Gimenez, Kevin J. Gaston, and David Mouillot. Taxonomic and regional uncertainty in species-area relationships and the identification of richness hotspots. *Proceedings of the National Academy of Sciences*, 105(40):15458–15463, October 2008. doi: 10.1073/pnas.0803610105.
- E. F. Connor and E. D. McCoy. Species–Area Relationships. In Simon A Levin, editor, *Encyclopedia of Biodiversity (Second Edition)*, pages 640–650. Academic Press, Waltham, January 2013. ISBN 978-0-12-384720-1. doi: 10.1016/B978-0-12-384719-5.00132-5.
- Luís Borda-de-Água, Paulo A. V. Borges, Stephen P. Hubbell, and Henrique M. Pereira. Spatial scaling of species abundance distributions. *Ecography*, 35(6):549–556, 2012. ISSN 1600-0587. doi: 10.1111/j.1600-0587.2011.07128.x.
- Matthew G. Betts, Lenore Fahrig, Adam S. Hadley, Katherine E. Halstead, Jeff Bowman, W. Douglas Robinson, John A. Wiens, and David B. Lindenmayer. A species-centered approach for uncovering generalities in organism responses to habitat loss and fragmentation. *Ecography*, 37(6):517–527, June 2014. ISSN 0906-7590, 1600-0587. doi: 10.1111/ecog.00740.
- Thomas J. Matthews, François Guilhaumon, Kostas A. Triantis, Michael K. Borregaard, and Robert J. Whittaker. On the form of species–area relationships in habitat islands and true islands. *Global Ecology and Biogeography*, 25(7): 847–858, 2016. ISSN 1466-8238. doi: 10.1111/geb.12269.
- Fangliang He and Pierre Legendre. Species Diversity Patterns Derived from Species–Area Models. *Ecology*, 83(5): 1185–1198, 2002. ISSN 1939-9170. doi: 10.1890/0012-9658(2002)083[1185:SDPDFS]2.0.CO;2.
- Patrick Weigelt and Holger Kreft. Quantifying island isolation – insights from global patterns of insular plant species richness. *Ecography*, 36(4):417–429, 2013. ISSN 1600-0587. doi: 10.1111/j.1600-0587.2012.07669.x.
- Thomas J. Matthews, François Rigal, Konstantinos Proios, Kostas A. Triantis, and Robert J. Whittaker. Explaining Variation in Island Species–Area Relationship (ISAR) Model Parameters between Different Archipelago Types: Expanding a Global Model of ISARs. In Thomas J. Matthews, Kostas A. Triantis, and Robert J. Whittaker, editors, *The Species–Area Relationship*, pages 51–77. Cambridge University Press, 1 edition, March 2021b. ISBN 978-1-108-56942-2 978-1-108-47707-9 978-1-108-70187-7. doi: 10.1017/9781108569422.007.

- Werner Ulrich, Thomas J. Matthews, Idoia Biurrun, Juan Antonio Campos, Patryk Czortek, Iwona Dembiczy, Franz Essl, Goffredo Filibeck, Gian-Pietro Giusso del Galdo, Behlül Güler, Alireza Naqinezhad, Péter Török, and Jürgen Dengler. Environmental drivers and spatial scaling of species abundance distributions in Palaearctic grassland vegetation. *Ecology*, 103(8):e3725, 2022. ISSN 1939-9170. doi: 10.1002/ecy.3725.
- Stina Drakare, Jack J. Lennon, and Helmut Hillebrand. The imprint of the geographical, evolutionary and ecological context on species–area relationships. *Ecology Letters*, 9(2):215–227, 2006. ISSN 1461-0248. doi: 10.1111/j.1461-0248.2005.00848.x.
- Katherine J. Willis and Robert J. Whittaker. Species Diversity–Scale Matters. *Science*, 295(5558):1245–1248, February 2002. doi: 10.1126/science.1067335.
- Will R. Turner and Even Tjørve. Scale-dependence in species-area relationships. *Ecography*, 28(6):721–730, 2005. ISSN 1600-0587. doi: 10.1111/j.2005.0906-7590.04273.x.
- J. A. Wiens. Spatial Scaling in Ecology. *Functional Ecology*, 3(4):385, 1989. ISSN 02698463. doi: 10.2307/2389612.
- K. A. Triantis, M. Mylonas, K. Lika, and K. Vardinoyannis. A model for the species–area–habitat relationship. *Journal of Biogeography*, 30(1):19–27, 2003. ISSN 1365-2699. doi: 10.1046/j.1365-2699.2003.00805.x.
- Athanasios S. Kallimanis, Antonis D. Mazaris, Joseph Tzanopoulos, John M. Halley, John D. Pantis, and Stefanos P. Sgardelis. How does habitat diversity affect the species–area relationship? *Global Ecology and Biogeography*, 17(4): 532–538, 2008. ISSN 1466-8238. doi: 10.1111/j.1466-8238.2008.00393.x.
- Attila Kalmar and David J. Currie. A Unified Model of Avian Species Richness on Islands and Continents. *Ecology*, 88(5):1309–1321, 2007. ISSN 1939-9170. doi: 10.1890/06-1368.
- William E. Kunin, John Harte, Fangliang He, Cang Hui, R. Todd Jobe, Annette Ostling, Chiara Polce, Arnošt Šizling, Adam B. Smith, Krister Smith, Simon M. Smart, David Storch, Even Tjørve, Karl-Inne Ugland, Werner Ulrich, and Varun Varma. Upscaling biodiversity: Estimating the species–area relationship from small samples. *Ecological Monographs*, 88(2):170–187, May 2018. ISSN 0012-9615, 1557-7015. doi: 10.1002/ecm.1284.
- Johanna Elena Schmitz and Sven Rahmann. A comprehensive review and evaluation of species richness estimation. *Briefings in Bioinformatics*, 26(2):bbaf158, March 2025. ISSN 1467-5463, 1477-4054. doi: 10.1093/bib/bbaf158.
- Jeanne Portier, Florian Zellweger, Jürgen Zell, Iciar Alberdi Asensio, Michal Bosela, Johannes Breidenbach, Vladimír Šebeň, Rafael O. Wüest, and Brigitte Rohner. Plot size matters: Toward comparable species richness estimates across plot-based inventories. *Ecology and Evolution*, 12(6), June 2022. ISSN 2045-7758, 2045-7758. doi: 10.1002/ece3.8965.
- Anne Chao, Nicholas J. Gotelli, T. C. Hsieh, Elizabeth L. Sander, K. H. Ma, Robert K. Colwell, and Aaron M. Ellison. Rarefaction and extrapolation with Hill numbers: A framework for sampling and estimation in species diversity studies. *Ecological Monographs*, 84(1):45–67, 2014. ISSN 1557-7015. doi: 10.1890/13-0133.1.
- Jorge Soberón M. and Jorge Llorente B. The Use of Species Accumulation Functions for the Prediction of Species Richness. *Conservation Biology*, 7(3):480–488, 1993. ISSN 1523-1739. doi: 10.1046/j.1523-1739.1993.07030480.x.
- Nicholas J. Gotelli and Robert K. Colwell. Quantifying biodiversity: Procedures and pitfalls in the measurement and comparison of species richness. *Ecology Letters*, 4(4):379–391, 2001. ISSN 1461-0248. doi: 10.1046/j.1461-0248.2001.00230.x.
- Milan Chytrý, Stephan M. Hennekens, Borja Jiménez-Alfaro, Ilona Knollová, Jürgen Dengler, Florian Jansen, Flavia Landucci, Joop H.J. Schaminée, Svetlana Ačić, Emiliano Agrillo, Didem Ambarlı, Pierangela Angelini, Iva Apostolova, Fabio Attorre, Christian Berg, Erwin Bergmeier, Idoia Biurrun, Zoltán Botta-Dukát, Henry Brisse, Juan Antonio Campos, Luis Carlón, Andraž Čarni, Laura Casella, János Csiky, Renata Čušterevska, Zora Dajić Stevanović, Jiří Danihelka, Els De Bie, Patrice de Ruffray, Michele De Sanctis, W. Bernhard Dickoré, Panayotis Dimopoulos, Dmytro Dubyna, Tetiana Dziuba, Rasmus Ejrnæs, Nikolai Ermakov, Jörg Ewald, Giuliano Fanelli, Federico Fernández-González, Úna

- FitzPatrick, Xavier Font, Itziar García-Mijangos, Rosario G. Gavilán, Valentin Golub, Riccardo Guarino, Rense Have-
man, Adrian Indreica, Deniz Işık Gürsoy, Ute Jandt, John A.M. Janssen, Martin Jiroušek, Zygmunt Kački, Ali Kav-
gacı, Martin Kleikamp, Vitaliy Kolomiychuk, Mirjana Krstivojević Čuk, Daniel Krstonošić, Anna Kuzemko, Jonathan
Lenoir, Tatiana Lysenko, Corrado Marcenò, Vassilij Martynenko, Dana Michalcová, Jesper Erenskjold Moeslund, Vik-
tor Onyshchenko, Hristo Pedashenko, Aaron Pérez-Haase, Tomáš Peterka, Vadim Prokhorov, Valerijus Rašomavičius,
Maria Pilar Rodríguez-Rojo, John S. Rodwell, Tatiana Rogova, Eszter Ruprecht, Solvita Rūsiņa, Gunnar Seidler, Jozef
Šibík, Urban Šilc, Željko Škvorc, Desislava Sopotlieva, Zvezdana Stančić, Jens-Christian Svenning, Grzegorz Swacha,
Ioannis Tsiripidis, Pavel Dan Turtureanu, Emin Uğurlu, Domas Uogintas, Milan Valachovič, Yulia Vashenyak, Kiril
Vassilev, Roberto Venanzoni, Risto Virtanen, Lynda Weekes, Wolfgang Willner, Thomas Wohlgemuth, and Sergey Ya-
malov. European Vegetation Archive (EVA): An integrated database of European vegetation plots. *Applied Vegetation
Science*, 19(1):173–180, 2016. ISSN 1654-109X. doi: 10.1111/avsc.12191.
- Patrick Weigelt, Christian König, and Holger Kreft. GIFT – A Global Inventory of Floras and Traits for macroecology
and biogeography. *Journal of Biogeography*, 47(1):16–43, 2020. ISSN 1365-2699. doi: 10.1111/jbi.13623.
- Edward F. Connor and Earl D. McCoy. The Statistics and Biology of the Species-Area Relationship. *The American
Naturalist*, 113(6):791–833, June 1979. ISSN 0003-0147, 1537-5323. doi: 10.1086/283438.
- Scott M Lundberg and Su-In Lee. A unified approach to interpreting model predictions. In I. Guyon, U. Von Luxburg,
S. Bengio, H. Wallach, R. Fergus, S. Vishwanathan, and R. Garnett, editors, *Advances in Neural Information Processing
Systems*, volume 30. Curran Associates, Inc., 2017.
- R H Whittaker. EVOLUTION AND MEASUREMENT OF SPECIES DIVERSITY. *TAXON*, 21(2-3):213–251, May
1972. ISSN 0040-0262. doi: 10.2307/1218190.
- Carsten Rahbek. The role of spatial scale and the perception of large-scale species-richness patterns. *Ecology Letters*, 8
(2):224–239, 2005. ISSN 1461-0248. doi: 10.1111/j.1461-0248.2004.00701.x.
- Anke Stein, Katharina Gerstner, and Holger Kreft. Environmental heterogeneity as a universal driver of species richness
across taxa, biomes and spatial scales. *Ecology Letters*, 17(7):866–880, 2014. ISSN 14610248. doi: 10.1111/ele.12277.
- Hong Qian and Robert E. Ricklefs. Disentangling the effects of geographic distance and environmental dissimilarity on
global patterns of species turnover. *Global Ecology and Biogeography*, 21(3):341–351, 2012. ISSN 1466-8238. doi:
10.1111/j.1466-8238.2011.00672.x.
- Richard Field, Bradford A. Hawkins, Howard V. Cornell, David J. Currie, J. Alexandre F. Diniz-Filho, Jean-François
Guégan, Dawn M. Kaufman, Jeremy T. Kerr, Gary G. Mittelbach, Thierry Oberdorff, Eileen M. O’Brien, and John
R. G. Turner. Spatial species-richness gradients across scales: A meta-analysis. *Journal of Biogeography*, 36(1):
132–147, 2009. ISSN 1365-2699. doi: 10.1111/j.1365-2699.2008.01963.x.
- Lirong Cai, Holger Kreft, Amanda Taylor, Pierre Denelle, Julian Schrader, Franz Essl, Mark Van Kleunen, Jan Pergl, Petr
Pyšek, Anke Stein, Marten Winter, Julie F. Barcelona, Nicol Fuentes, Inderjit, Dirk Nikolaus Karger, John Kartesz,
Andrej Kuprijanov, Misako Nishino, Daniel Nickrent, Arkadiusz Nowak, Annette Patzelt, Pieter B. Pelser, Paramjit
Singh, Jan J. Wieringa, and Patrick Weigelt. Global models and predictions of plant diversity based on advanced
machine learning techniques. *New Phytologist*, 237(4):1432–1445, February 2023. ISSN 0028-646X, 1469-8137. doi:
10.1111/nph.18533.
- Alexandre Antonelli, W. Daniel Kissling, Suzette G.A. Flantua, Mauricio A. Bermúdez, Andreas Mulch, Alexandra N.
Muellner-Riehl, Holger Kreft, H. Peter Linder, Catherine Badgley, Jon Fjeldså, Susanne A. Fritz, Carsten Rahbek,
Frédéric Herman, Henry Hooghiemstra, and Carina Hoorn. Geological and climatic influences on mountain biodiver-
sity. *Nature Geoscience*, 11(10):718–725, 2018. ISSN 17520908. doi: 10.1038/s41561-018-0236-z.
- Philipp Brun, Dirk N. Karger, Damaris Zurell, Patrice Descombes, Lucienne C. de Witte, Riccardo de Lutio, Jan Dirk
Wegner, and Niklaus E. Zimmermann. Multispecies deep learning using citizen science data produces more in-
formative plant community models. *Nature Communications*, 15(1):4421, May 2024. ISSN 2041-1723. doi:
10.1038/s41467-024-48559-9.

- Shawn J. Leroux, Cécile H. Albert, Anne-Sophie Lafuite, Bronwyn Rayfield, Shaopeng Wang, and Dominique Gravel. Structural uncertainty in models projecting the consequences of habitat loss and fragmentation on biodiversity. *Ecography*, 40(1):36–47, 2017. ISSN 1600-0587. doi: 10.1111/ecog.02542.
- Anne Dubuis, Julien Pottier, Vanessa Rion, Loïc Pellissier, Jean-Paul Theurillat, and Antoine Guisan. Predicting spatial patterns of plant species richness: A comparison of direct macroecological and species stacking modelling approaches. *Diversity and Distributions*, 17(6):1122–1131, 2011. ISSN 1472-4642. doi: 10.1111/j.1472-4642.2011.00792.x.
- Stephen P Hubbell. *The Unified Neutral Theory of Biodiversity and Biogeography*. Princeton University press, Princeton [etc, 2001. ISBN 0-691-02128-7.
- Jon C. Gering, Thomas O. Crist, and Joseph A. Veech. Additive Partitioning of Species Diversity across Multiple Spatial Scales: Implications for Regional Conservation of Biodiversity. *Conservation Biology*, 17(2):488–499, 2003. ISSN 1523-1739. doi: 10.1046/j.1523-1739.2003.01465.x.
- Chris D. Thomas, Alison Cameron, Rhys E. Green, Michel Bakkenes, Linda J. Beaumont, Yvonne C. Collingham, Barend F. N. Erasmus, Marinez Ferreira de Siqueira, Alan Grainger, Lee Hannah, Lesley Hughes, Brian Huntley, Albert S. van Jaarsveld, Guy F. Midgley, Lera Miles, Miguel A. Ortega-Huerta, A. Townsend Peterson, Oliver L. Phillips, and Stephen E. Williams. Extinction risk from climate change. *Nature*, 427(6970):145–148, January 2004. ISSN 1476-4687. doi: 10.1038/nature02121.
- Thomas M. Brooks, Russell A. Mittermeier, Cristina G. Mittermeier, Gustavo A. B. Da Fonseca, Anthony B. Rylands, William R. Konstant, Penny Flick, John Pilgrim, Sara Oldfield, Georgina Magin, and Craig Hilton-Taylor. Habitat Loss and Extinction in the Hotspots of Biodiversity. *Conservation Biology*, 16(4):909–923, 2002. ISSN 1523-1739. doi: 10.1046/j.1523-1739.2002.00530.x.
- Jacob B. Socolar, James J. Gilroy, William E. Kunin, and David P. Edwards. How Should Beta-Diversity Inform Biodiversity Conservation? *Trends in Ecology & Evolution*, 31(1):67–80, January 2016. ISSN 0169-5347. doi: 10.1016/j.tree.2015.11.005.
- Marc-André Carbonneau, Veronika Cheplygina, Eric Granger, and Ghyslain Gagnon. Multiple instance learning: A survey of problem characteristics and applications. *Pattern Recognition*, 77:329–353, May 2018. ISSN 00313203. doi: 10.1016/j.patcog.2017.10.009.
- Maximilian Ilse, Jakub M. Tomczak, and Max Welling. Attention-based Deep Multiple Instance Learning, June 2018.
- Ilkka Hanski, Gustavo A. Zurita, M. Isabel Bellocq, and Joel Rybicki. Species–fragmented area relationship. *Proceedings of the National Academy of Sciences*, 110(31):12715–12720, July 2013. doi: 10.1073/pnas.1311491110.
- Joel Rybicki and Ilkka Hanski. Species–area relationships and extinctions caused by habitat loss and fragmentation. *Ecology Letters*, 16(s1):27–38, 2013. ISSN 1461-0248. doi: 10.1111/ele.12065.
- Iwona Dembicz, Jürgen Dengler, Manuel J. Steinbauer, Thomas J. Matthews, Sándor Bartha, Sabina Burrascano, Alessandro Chiarucci, Goffredo Filibeck, François Gillet, Monika Janišová, Salza Palpurina, David Storch, Werner Ulrich, Svetlana Ačić, Steffen Boch, Juan Antonio Campos, Laura Cancellieri, Marta Carboni, Giampiero Ciaschetti, Timo Conradi, Pieter De Frenne, Jiri Dolezal, Christian Dolnik, Franz Essl, Edy Fantinato, Itziar García-Mijangos, Gian Pietro Giusso del Galdo, John-Arvid Grytnes, Riccardo Guarino, Behlül Güler, Jutta Kapfer, Ewelina Kli-chowska, Łukasz Kozub, Anna Kuzemko, Swantje Löbel, Michael Manthey, Corrado Marcenò, Anne Mimet, Alireza Naqinezhad, Jalil Noroozi, Arkadiusz Nowak, Harald Pauli, Robert K. Peet, Vincent Pellissier, Remigiusz Pielech, Massimo Terzi, Emin Uğurlu, Orsolya Valkó, Iuliia Vasheniak, Kiril Vassilev, Denys Vynokurov, Hannah J. White, Wolfgang Willner, Manuela Winkler, Sebastian Wolfrum, Jinghui Zhang, and Idoia Biurrun. Fine-grain beta diversity of Palaearctic grassland vegetation. *Journal of Vegetation Science*, 32(3):e13045, 2021. ISSN 1654-1103. doi: 10.1111/jvs.13045.
- GBIF: The Global Biodiversity Information Facility. What is GBIF? 2022.

- H. De Kort, J. G. Prunier, S. Ducatez, O. Honnay, M. Baguette, V. M. Stevens, and S. Blanchet. Life history, climate and biogeography interactively affect worldwide genetic diversity of plant and animal populations. *Nature Communications*, 12(1):516, January 2021. ISSN 2041-1723. doi: 10.1038/s41467-021-20958-2.
- Robert K. Colwell, Jonathan A. Coddington, and David L. Hawksworth. Estimating terrestrial biodiversity through extrapolation. *Philosophical Transactions of the Royal Society of London. Series B: Biological Sciences*, 345(1311): 101–118, January 1997. doi: 10.1098/rstb.1994.0091.
- Yi Zou, Peng Zhao, and Jan Christoph Axmacher. Estimating total species richness: Fitting rarefaction by asymptotic approximation. *Ecosphere*, 14(1):e4363, January 2023. ISSN 2150-8925, 2150-8925. doi: 10.1002/ecs2.4363.
- Jürgen Dengler and Jens Oldeland. Effects of sampling protocol on the shapes of species richness curves. *Journal of Biogeography*, 37(9):1698–1705, September 2010. ISSN 0305-0270, 1365-2699. doi: 10.1111/j.1365-2699.2010.02322.x.
- Diederik P. Kingma and Jimmy Ba. Adam: A Method for Stochastic Optimization. pages 1–15, December 2014.
- Ilya Loshchilov and Frank Hutter. Decoupled Weight Decay Regularization, January 2019.
- Philipp Brun, Niklaus E. Zimmermann, Chantal Hari, Loïc Pellissier, and Dirk Nikolaus Karger. Global climate-related predictors at kilometer resolution for the past and future. *Earth System Science Data*, 14(12):5573–5603, December 2022. ISSN 1866-3508. doi: 10.5194/essd-14-5573-2022.

S1 Supplementary materials

Derivation of the Michaelis-Menten model from the exponential distribution. Assuming the species density distribution follows an exponential distribution $f(\lambda) = \beta e^{-\beta\lambda}$ for $\lambda > 0$, where $\beta > 0$ is a parameter, then the Laplace transform of $f(\lambda)$ is $\mathcal{L}\{f\}(s) = \int_0^\infty e^{-s\lambda} \beta e^{-\beta\lambda} d\lambda = \beta \int_0^\infty e^{-\lambda(s+\beta)} d\lambda = \frac{\beta}{s+\beta}$. Substituting this into Eq. (3) gives $\mathbb{E}[S_{\text{obs}}(m)] = S_{\text{tot}} \left(1 - \frac{\beta}{A(m)+\beta}\right) = S_{\text{tot}} \frac{A(m)}{A(m)+\beta}$ which recovers the Michaelis-Menten formula, commonly used for estimating rarefaction curves (Colwell et al., 1997; Dengler, 2009).

S2 Supplementary figures

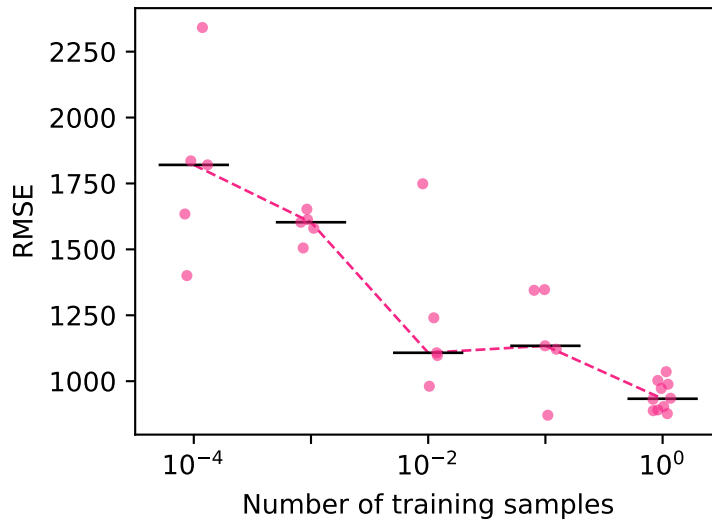


Figure S5: **Model's performance in predicting the EVA-based test dataset against the proportion of generated training samples relative to the number of surveys.** These results demonstrate that the optimal number of training data samples, generated through random pooling of vegetation plots, is on the order of magnitude of the number of surveys.

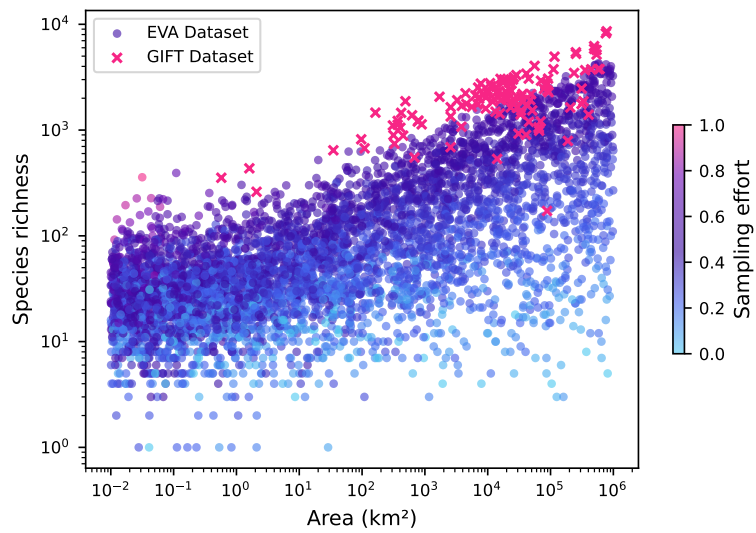


Figure S6: **Species richness against habitat area and sampling effort, for the EVA-based and GIFT-based datasets.** The sampling effort is calculated as the ratio of the logarithm of observed area over the logarithm of the habitat area.

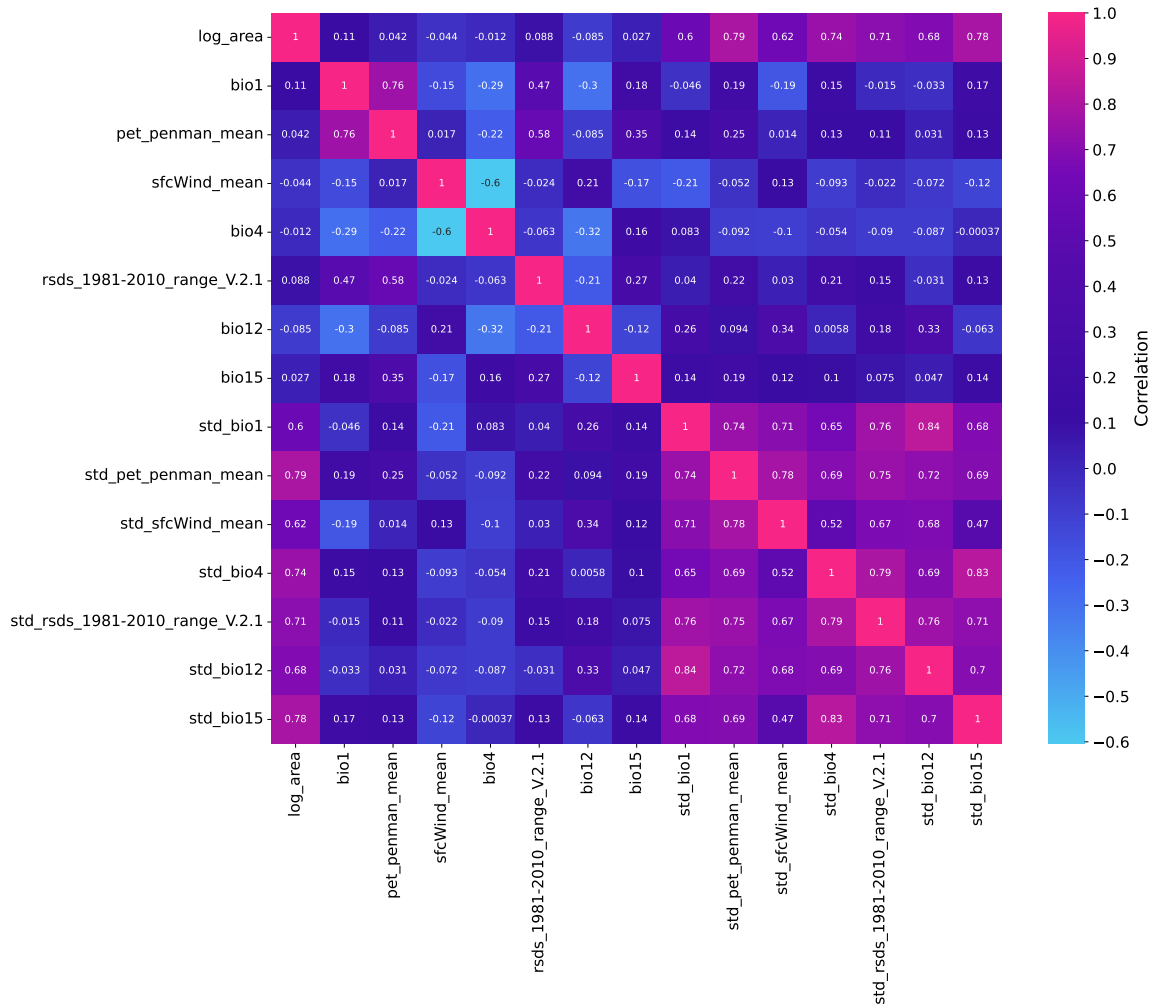


Figure S7: Correlation matrix of environmental features associated to the EVA-dataset.

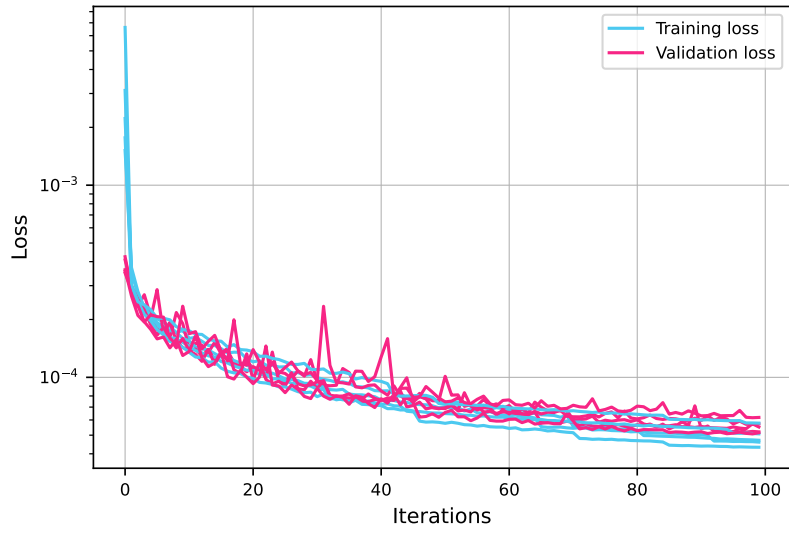


Figure S8: Training and validation loss against the number of epochs for each member of the deep SAR ensemble model trained with area and climate features.

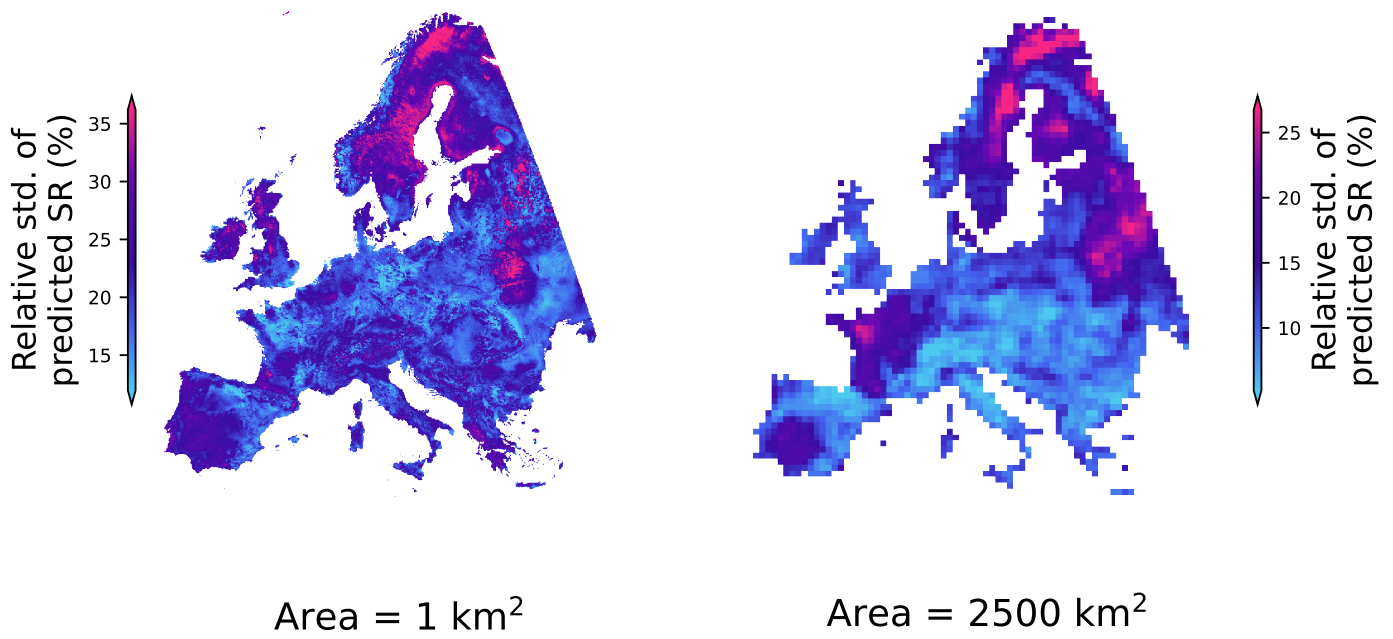


Figure S9: Relative standard deviation of the predictions obtained from the deep SAR ensemble model and displayed in Fig. 4.

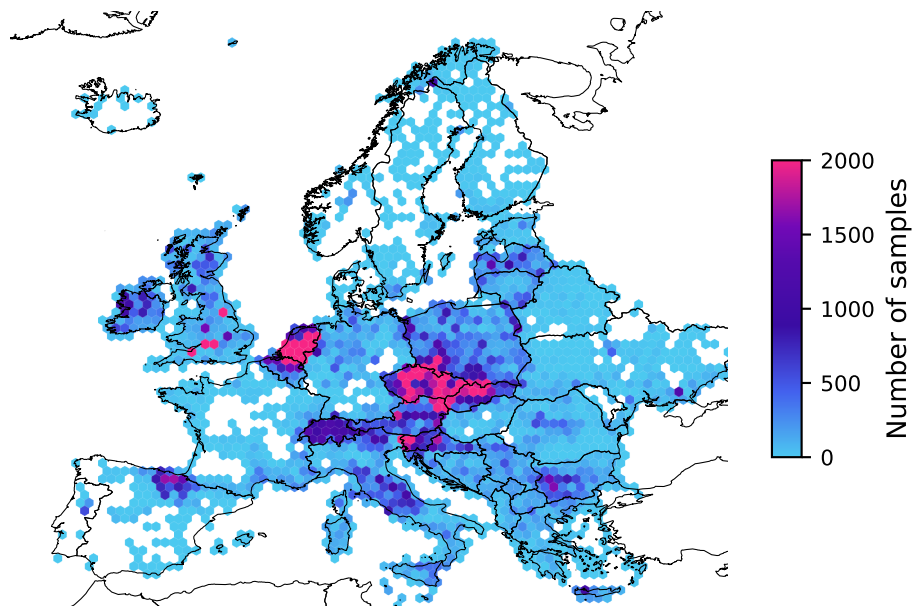


Figure S10: Density of EVA vegetation plots (number of samples per hexagon with width of 50km).